RAP CONFERENCE PROCEEDINGS, VOL. 10, PP. 54–58, 2025
ISSN 2737-9973 (ONLINE) | DOI: 10.37392/RAPPROC.2025.11
RAP-PROCEEDINGS.ORG

# A NEW PERSONAL ELECTRONIC DOSIMETER: THE PDOZ

**Lucia Salvi[1,2,3*], Ali Behcet Alpat[1], Giovanni Bartolini[1,3], Marco Bizzarri[2], Andrea Papi[1], Leonello Servoli[1], Haider Raheem[3]**

[1]National Institute for Nuclear Physics (INFN), Section of Perugia, Perugia, Italy
[2]Departement of Physics and Geology, University of Perugia, Perugia, Italy
[3]BEAMIDE srl, Perugia, Italy

***Abstract.*** *The PDOZ is a personal electronic dosimeter designed to measure exposure to ionizing radiation in environments such as research laboratories, hospitals, and nuclear facilities. Its aim is to detect, discriminate, and measure the dose and dose rate from beta particles, gamma rays, and neutrons in real-time in mixed radiation fields of unknown sources. The device features three scintillators: a thin BC408 for beta particles, a thick BC408 for neutrons, and the CsI(Tl) for gamma rays. At the bottom surface of each scintillator, two silicon photomultipliers (SiPMs) are attached to a total of six SiPMs. Geant4 simulations were used to optimize the materials and thicknesses of the scintillators. Preliminary experimental measurements with $^{90}$Sr, $^{60}$Co and $^{137}$Cs sources show good agreement with the simulations for the single scintillator PDOZ configuration based on BC408. Further comparisons between simulated and experimental results for $^{90}$Sr, $^{60}$Co and $^{137}$Cs, as well as neutron detection efficiency tests, are ongoing with the complete geometry of the PDOZ.*

***Keywords:*** *beta particles, dose rate, gamma rays, ionizing radiation, neutrons, PDOZ, personal electronic dosimeter, scintillators, silicon photomultipliers, simulation*

## 1. INTRODUCTION

The PDOZ [1] is an R&D project of BEAMIDE srl [2] in collaboration with the National Institute of Nuclear Physics (INFN) and the Department of Physics and Geology of Perugia University. It is a multipurpose personal electronic dosimeter developed to perform measurements in mixed radiation fields of unknown sources. Its purpose is to detect, discriminate, and measure the dose and dose rate provided by gamma rays, beta particles, and neutrons in real time. For this reason, three distinct scintillators, each specific to a given kind of particle, are inside the PDOZ. There is a crystal scintillator, the CsI(Tl) [3], to detect gamma rays, and two plastic scintillators made of BC408 [4] each with different thicknesses. The thin BC408 is used to detect beta particles, while the thicker BC408 is used for neutron detection. Two SiPMs are attached to the bottom surface of each scintillator for a total of six SiPMs. A count is recorded when both SiPMs on the same scintillator have a pulse over threshold in coincidence. This coincidence requirement suppresses false events caused by thermally generated free charge carriers, reducing thermal noise to approximately $10^{-3}$ Hz.

Like any other personal dosimeter on the market, the PDOZ must meet certain requirements, such as those specified by the International Electrotechnical Commission, IEC 61526:2010 [5], which outlines general characteristics, test procedures and radiation characteristics, along with electrical, mechanical, safety, and environmental criteria. The PDOZ must be able to detect gamma rays over a wide energy range, from 20 keV up to 1250 keV, with a measurement uncertainty within 30% when referred to the $^{137}$Cs emission (~660 keV). For gamma rays with energies equal to or greater than 6 MeV, the measurement uncertainty must be within 50%, when referred to $^{137}$Cs gamma rays. For beta particles, the detectable energy range is from 200 keV to 2.5 MeV, with a measurement uncertainty within 30% when referred to a $^{90}$Sr/$^{90}$Y source. For neutrons, the detectable energy range extends from 25 meV to 15 MeV, with a personal dose equivalent accuracy of 10% when referred to an AmBe source. Regarding the angular response, the maximum signal reduction must not exceed 20% up to 60° from normal incidence.

## 2. CONVERSION CURVES

To calculate the dose and dose rate, it is necessary to evaluate the conversion curve that transforms the count per second (CPS) into μSv/h. This estimation requires two different simulations, both implemented using the Geant4 toolkit [6]. The first simulation models the ICRU sphere [7], while the second one simulates the dosimeter itself.

### *2.1. ICRU sphere*

The ICRU sphere is a sphere with a unity density, 1 g/cm$^3$, with a diameter of 30 cm, and it is made of

* lucia.salvi@pg.infn.it

tissue-equivalent material, thus 76.2% oxygen; 11.1% carbon; 10.1% hydrogen; and 2.6% nitrogen. This simulation is used to calculate the fluence-to-dose equivalent conversion coefficients. Inside the sphere, a sensitive cube made of the same tissue-equivalent material is placed at a specific distance from the sphere's surface, depending on the type of incoming radiation. For low-penetrating radiation such as beta particles, the sensitive cube is positioned near the sphere's surface. For more penetrating radiations, such as gamma rays and neutrons, the cube is located deeper within the sphere.

To determine the fluence-to-dose equivalent conversion coefficients, beams composed of only one type of particles are simulated, and their fluences are calculated by dividing the number of generated events by the source area. Subsequently, the fluence-to-dose equivalent conversion coefficients [8] are calculated by dividing the dose by the fluence as shown in equation (1):

$$X(E) = D/F \qquad (1)$$

where *X(E)* is the fluence-to-dose equivalent conversion coefficients (measured in pSV·cm² for gamma rays and in nSv·cm² for beta particles), *D* is the dose and *F* is the fluence.

### 2.2. Dosimeter Response

To study the dosimeter response, the PDOZ is simulated with a circular source emitting a single type of particle. The dosimeter response is found by dividing the number of events with two SiPMs in coincidence by the fluence as shown in equation (2):

$$R(E) = n_c/F \qquad (2)$$

where *R(E)* denotes the dosimeter response, $n_c$ is the number of events detected in coincidences by the two SiPMs and *F* represents the fluence.

Finally, the conversion factors for the conversion curve, expressed in µSv/CPS·h, are calculated using equation (3):

$$CF(E) = X(E)/R(E) \qquad (3)$$

where *CF(E)* are the conversion factors, *X(E)* are the fluence-to-ambient-dose equivalent conversion coefficients and *R(E)* is the dosimeter response.

## 3. Detector

The PDOZ contains three distinct scintillators, one CsI(Tl) and two BC408 with two different thicknesses. The CsI(Tl) scintillator, used for gamma ray detection, and the thick BC408 block, employed for neutron detection, are both cubic samples with 10 mm sides. The thin BC408 scintillator, used for beta particle detection, has the same lateral dimensions as the others but is 1.5 mm thick. All three scintillators are positioned at the same height inside the external box, along with their associated electronic circuitry. Coupled to the bottom of each scintillator, two J-Series Onsemi [9] SiPMs are attached to detect the light produced by incoming particles.

Three different acquisition system conditions are implemented:

- p.e.0, at least one optical photon must reach each SiPM;
- p.e.1, at least two optical photons must arrive at each SiPM;
- p.e.2, three optical photons must arrive at each SiPM.

A count is registered whenever signals from both SiPMs on a given scintillator coincide within the same event.

### 3.1. Single Scintillator PDOZ

The first tests were performed on a single scintillator dosimeter, with the BC408 scintillator chosen, having dimensions of 10 x 5 x 15 mm³. Both the scintillator and the radioactive sources used in the laboratory were simulated, with the distance between the scintillator and the source varied from 0.5 to 5 cm. In this way, a comparison between simulation results and experimental data can be performed. To study the single scintillator dosimeter response to beta particles, a $^{90}$Sr source was used, while $^{60}$Co and $^{137}$Cs sources were employed for gamma ray response. The comparisons between experimental data and Monte Carlo simulations are presented in Figures 1, 2, and 3.

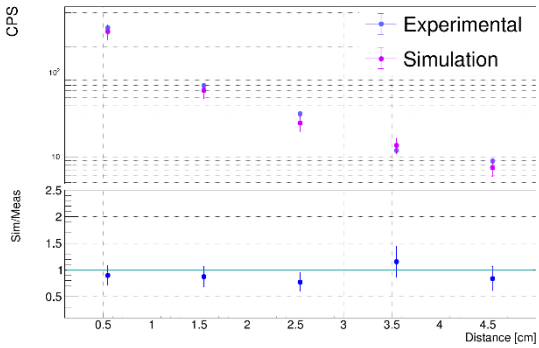


Figure 1. Comparison between simulated and experimental data with a $^{90}$Sr source. The blue points denote the ratio between simulated and experimental data. The ratio demonstrates good agreement between simulation and experimental results, while the observed deviations are due to the unstable experimental setup, which prevented perfect alignment between the source and the scintillator [1].

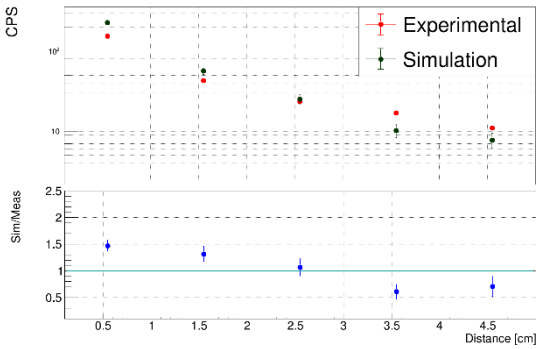


Figure 2. Comparison between simulated and experimental data with a $^{60}$Co source. The blue points denote the ratio between simulated and experimental data. The ratio demonstrates good agreement between simulation and experimental results, while the observed deviations are due to the unstable experimental setup, which prevented perfect alignment between the source and the scintillator [1].

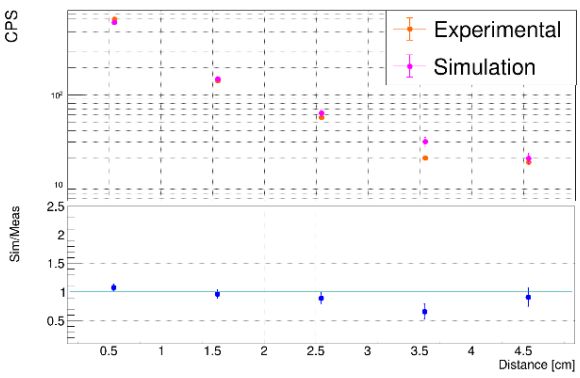


Figure 3. Comparison between simulated and experimental data with a $^{137}$Cs source. The blue points denote the ratio between simulated and experimental data. The ratio demonstrates good agreement between simulation and experimental results, while the observed deviations are due to the unstable experimental setup, which prevented perfect alignment between the source and the scintillator [1].

The data obtained in the laboratory show quite good agreement with the simulation results. The discrepancies are mainly due to an unstable experimental setup, which caused the alignment between the radioactive source and the scintillator to be less than optimal.

## 4. Scintillator Simulations

After the single scintillator dosimeter test, simulations were carried out to identify the best scintillator candidates for detecting gamma rays and neutrons.

### *4.1. Gamma Rays Scintillator*

Several types of crystal scintillators were simulated with a cubic geometry of 10 mm per side, CsI [3], CsI(Na) [3], CsI(Tl), and GAGG [10]. To study their gamma ray detection efficiency, all the scintillators' physical and optical properties were implemented inside the simulation, and the results are shown in Figure 4.

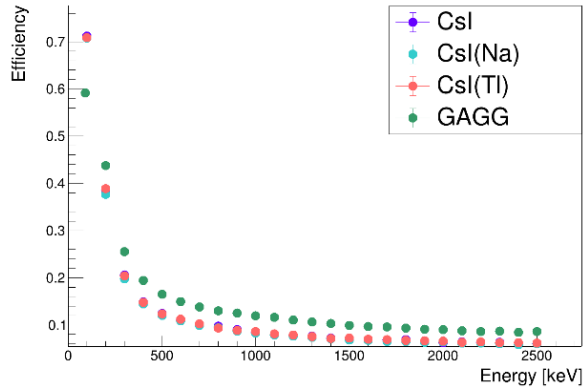


Figure 4. Gamma ray detection efficiency of CsI, CsI(Na), CsI(Tl), and GAGG scintillators as a function of energy. The CsI, CsI(Na) and CsI(Tl) points overlapped. All scintillators exhibit similar behavior, with efficiencies generally higher at low energies.

From the results obtained, all scintillators demonstrated good gamma ray detection efficiency. However, the CsI(Tl) and CsI(Na) were selected due to their good detection efficiency. Notably, CsI(Na) has a maximum emission wavelength at 420 nm, which is well compatible with the peak of the photon detection efficiency wavelength of the SiPMs used, J-Series Onsemi. Although GAGG exhibits the best gamma-ray detection efficiency, it was not chosen because its maximum emission wavelength is 520 nm, which is not compatible with the peak photon detection efficiency wavelength of the SiPMs.

### *4.2. Neutrons Scintillator*

To identify the most suitable scintillator candidates for neutron detection, several simulations were carried out using different types of scintillators and various geometrical configurations. The neutron physics simulations were performed using the NeutronHP package in Geant4.

The simulated geometrical configurations were:

- SCINTILLATOR: only the scintillator of dimensions 10 x 10 x 15 mm$^3$;
- SCINTILLATOR and MODERATOR: a moderator of polyethylene with a thickness of 1.50 mm is put in front of the scintillator;
- SCINTILLATOR, CONVERTER and MODERATOR (Boron): a converter of $^{10}$B with a thickness of 1.50 mm is inserted between the moderator and the scintillator;
- SCINTILLATOR, CONVERTER and MODERATOR (Lithium): a converter made of $^{6}$Li, 1.50 mm thick, is placed between the moderator and the scintillator.

The simulated scintillators were plastics, crystals, and glass. Firstly, the detection efficiency for neutrons at 1 MeV was studied to determine the best geometrical configuration and to select the five best scintillator candidates that are shown in Table 1.

Table 1. Five best scintillator candidates and their optimal geometrical configuration for maximum efficiency in detecting 1 MeV neutrons.

| Scintillators | Configuration | Max efficiency @ 1 MeV |
|---|---|---|
| BC408 | Only scint | 0.047 |
| EJ-254 | Only scint | 0.032 |
| EJ-276D | Only scint | 0.031 |
| CLLBC | Only scint | 0.014 |
| GAGG | Only scint | 0.011 |

The selected geometrical configuration is the one with only the scintillator implemented, while the selected scintillators are three plastics, BC408, EJ-254 [11], and EJ-276D [12]; and two crystals, CLLBC [13] and GAGG.

After the selection of the geometrical configuration and the scintillator candidates, neutron detection efficiency was studied inside the energy range of

[~$10^{-3}$ - 15] MeV. The results obtained are shown in Figure 5.

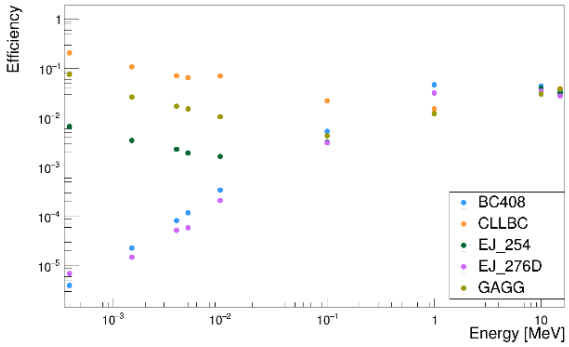


Figure 5. Neutron detection efficiency of BC408, CLLBC, EJ-254, EJ-276D, and GAGG scintillators as a function of energy, obtained from simulations. At high energies, all scintillators exhibit similar behavior, while at low energies the highest efficiencies are observed for CLLBC, GAGG, and EJ-254.

The results show a similar detection efficiency behavior in BC408, EJ-276D, and EJ-254 scintillators because they are all plastics. Only the EJ-254 scintillator has better detection efficiency at lower energy because it contains nearly 1% of $^{10}$B. The detection efficiencies of CLLBC and GAGG scintillators are good because they both contain elements with a good cross section for neutron capture. More details, in CLLBC scintillator, the fast neutrons can be detected because of $^{35}$Cl and $^{6}$Li, while thermal neutrons are detected because of $^{6}$Li, $^{133}$Cs, $^{79,81}$Br and $^{35,37}$Cl. Inside the GAGG, instead, thermal neutrons are detected thanks to $^{157}$Gd. However, CLLBC contains lanthanum. If a neutron interacts with lanthanum, some of its radioactive isotopes can be produced, thus it is not suitable to be used inside a personal electronic dosimeter. Concerning the GAGG scintillator, instead, it has also good gamma ray detection efficiency, thus there will be contamination from gammas.

For these reasons, the chosen scintillators are EJ-254 and BC408.

## 5. First PDOZ Prototype Simulation and Construction

Following the selection of the most appropriate scintillators for each particle type, a simulation was conducted on the first full prototype, incorporating all three scintillators integrated within its structure.

The PDOZ geometry was designed using CAD software [14] and saved in STEP file format, which was then converted to the GDML file format using the MRADSIM CONVERTER R software [15]. This allowed the geometry to be imported from the GDML file within Geant4, where the optical properties of the materials were defined and assigned to each specific component of the geometry. In this way, the performance of the dosimeter was studied, the conversion curves for all three particle kinds were determined, and the first dose rate study from the CPS was implemented.

As an example, the conversion curve of the CsI(Tl) scintillator for gamma rays is presented in Figure 6.

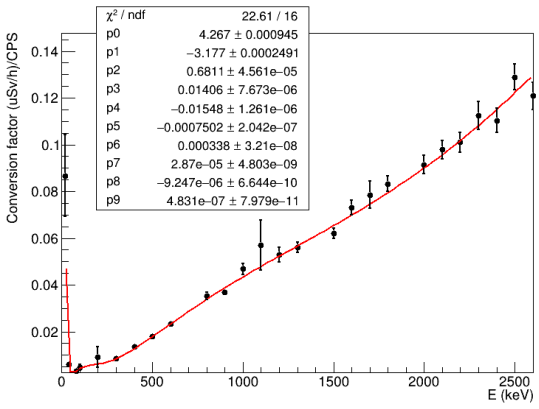


Figure 6. CsI(Tl) conversion curve for gamma rays as a function of energy, obtained from simulations. The black points represent the calculated conversion factors, while the red curve is used to convert counts per second into dose rate.

By multiplying the conversion coefficients by the CPS, the dose rate as a function of energy is obtained, as shown in Figure 7.

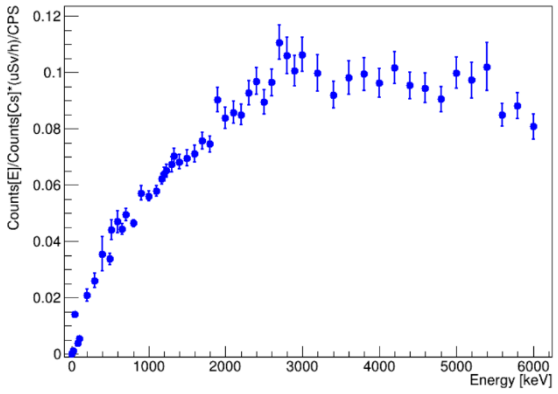


Figure 7. Preliminary dose rate estimation from conversion factors and CPS.

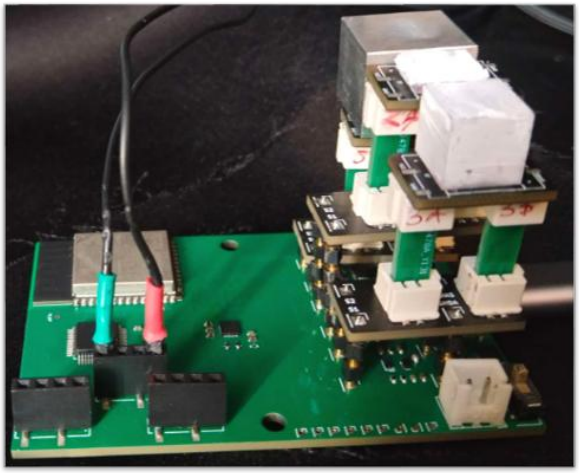

Figure 8. Internal configuration of the PDOZ. The cube covered with metal foil is the CsI(Tl) scintillator, followed by the thin BC408 scintillator in the middle, and the thicker BC408 scintillator positioned closest to the viewer.

After simulations of the first PDOZ prototype, a preliminary device was fabricated with its internal configuration depicted in Figure 8.

Up to now, the dark counts for each scintillator were determined to evaluate the threshold levels necessary to eliminate the irrelevant counts. Furthermore, the initial tests were conducted using $^{90}$Sr and $^{60}$Co radioactive sources, while experiments with $^{137}$Cs, $^{252}$Cf and AmBe sources are planned, along with a data acquisition campaign on a neutron beam.

## 6. Conclusion

The simulations not only closely replicate the experimental setup and the relevant physical processes, but the initial data collected using the single scintillator PDOZ also show reasonable agreement with the simulation results. This validates both the Monte Carlo approach and the selected physical parameters. These findings suggest that PDOZ, in its final configuration, has the potential to provide real-time detection, discrimination, and measurement of dose and dose rate for gamma rays, beta particles, and neutrons. In the future, PDOZ can be deployed in hospitals, research laboratories, and nuclear facilities to support routine radiation monitoring and enhance personnel safety in mixed or unknown radiation fields.

## References


1. L. Salvi et al., "PDOZ: innovative personal electronic dosimeter for electron and gamma H*(d) dosimetry," *J. Instrum.*, vol. 18, no. 8, P08010, Aug. 2023. DOI: 10.1088/1748-0221/18/08/P08010
2. *BEAMIDE*, INFN, Perugia, Italy, 2021. Retrieved from: https://www.beamide.com Retrieved on: Jul. 16, 2025
3. *Scintillators Model CsI(Tl), CsI(Na) and pure CsI datasheet*, Epic-Crystal, Kunshan, China, 2012. Retrieved from: https://www.epic-crystal.com/scintillation-crystals/csi-crystal.html Retrieved on: Jul. 16, 2025
4. *Scintillator Model BC408 datasheet*, Luxium Solutions, Hiram (OH), USA. Retrieved from: https://www.luxiumsolutions.com/radiation-detection-scintillators/plastic-scintillators/bc400-bc404-bc408-bc412-bc416 Retrieved on: Jul. 16, 2025
5. *Radiation protection instrumentation – Measurement of personal dose equivalents Hp(10) and Hp(0,07) for X, gamma, neutron and beta radiations – Direct reading personal dose equivalent meters*, IEC 61526:2010, Jul. 22, 2010. Retrieved from: https://webstore.iec.ch/en/publication/5540 Retrieved on: Jul. 16, 2025
6. S. Agostinelli et al., *Geant4 simulation toolkit version 10.7*, CERN, Geneva, Switzerland, 2020. Retrieved from: https://geant4.web.cern.ch/ Retrieved on: Jul. 16, 2025.
7. *Determination of dose equivalent resulting from external radiation sources*, Rep. 39, ICRU, Bethesda (MD), USA, 1985. Retrieved from: https://www.icru.org/report/determination-of-dose-equivalents-resulting-from-external-radiation-sources-report-39/ Retrieved on: Jul. 16, 2025
8. *Conversion coefficients for use in radiological protection against external radiation*, ICRP Publication 74, ICRP, Oxford (UK), 1996. Retrieved from: https://www.icrp.org/publication.asp?id=icrp%20publication%2074 Retrieved on: Jul. 16, 2025
9. *J-Series Silicon Photomultiplier (SiPM) Sensors datasheet*, Onsemi, Scottsdale (AZ), USA. Retrieved from: https://www.onsemi.com/products/sensors/photodetectors-sipm-spad/silicon-photomultipliers-sipm/j-series Retrieved on: Jul. 16, 2025
10. *GAGG Scintillator datasheet*, Advatech, London, UK. Retrieved from: https://www.advatech-uk.co.uk/gagg_ce.html Retrieved on: Jul. 16, 2025
11. *EJ-254 Scintillator datasheet*, Eljen Technology, Sweetwater (TX), USA. Retrieved from: https://eljentechnology.com/images/products/datasheets/EJ-254.pdf Retrieved on: Jul. 16, 2025
12. *EJ-276D and EJ-276G Scintillators datasheet*, Eljen Technology, Sweetwater (TX), USA. Retrieved from: https://eljentechnology.com/products/plastic-scintillators/ej-276 Retrieved on: Jul. 16, 2025
13. *CLLBC Scintillator datasheet*, Berkeley Nucleonics Corp, San Rafael (CA), USA. Retrieved from: http://www.berkeleynucleonics.com/sites/default/files/products/resources/cllbc_datasheet_bnc.pdf Retrieved on: Jul. 16, 2025
14. *AutoCAD version 2023*, Autodesk, Inc., San Rafael (CA), USA, 2023. Retrieved from: https://www.autodesk.com/products/autocad/overview Retrieved on: Jul. 16, 2025
15. *MRADSIM Converter*, MRADSIM, Perugia, Italy, 2023. Retrieved from: https://www.mradsim.com/converter Retrieved on: Jul. 16, 2025